

Spiking Neural Networks for Fast-Moving Object Detection on Neuromorphic Hardware Devices Using an Event-Based Camera

Andreas Ziegler, Karl Vetter, Thomas Gossard, Jonas Tebbe, and Andreas Zell

Abstract—Table tennis is a fast-paced and exhilarating sport that demands agility, precision, and fast reflexes. In recent years, robotic table tennis has become a popular research challenge for robot perception algorithms. Fast and accurate ball detection is crucial for enabling a robotic arm to rally the ball back successfully. Previous approaches have employed conventional frame-based cameras with Convolutional Neural Networks (CNNs) or traditional computer vision methods. In this paper, we propose a novel solution that combines an event-based camera with Spiking Neural Networks (SNNs) for ball detection. We use multiple state-of-the-art SNN frameworks and develop a SNN architecture for each of them, complying with their corresponding constraints. Additionally, we implement the SNN solution across multiple neuromorphic edge devices, conducting comparisons of their accuracies and run-times. This furnishes robotics researchers with a benchmark illustrating the capabilities achievable with each SNN framework and a corresponding neuromorphic edge device. Next to this comparison of SNN solutions for robots, we also show that an SNN on a neuromorphic edge device is able to run in real-time in a closed loop robotic system, a table tennis robot in our use case.

SUPPLEMENTARY MATERIAL

Additional resources are available at: <https://cogsys-tuebingen.github.io/snn-edge-benchmark>

I. INTRODUCTION

In recent years, robotic table tennis has become a popular research challenge for perception and robot control. While not yet able to compete with professional players, table tennis robots are an exciting research environment to bring perception and control algorithms towards their limits [1]. Fast and accurate ball detection is a crucial perception task for a table tennis robot system. So far, most research uses frame-based cameras together with a Convolutional Neural Network (CNN) based ball detection or a classical computer vision approach [2][3][4][5]. In this work, we enter a different avenue and combine two more recent technologies, event-based cameras and Spiking Neural Networks (SNNs).

SNNs mimic the spiking behavior of biological neurons, offering a biologically inspired approach to Neural Network (NN) computation. Unlike traditional artificial neurons that produce real-valued outputs, spiking neurons receive input spikes and integrate them in the state of the neuron, called membrane potential. When the neuron’s membrane potential reaches a defined threshold, the neuron emits a spike that propagates through the network, and resets its membrane

The authors are with the Cognitive Systems Group, Department of Computer Science, University of Tübingen. Corresponding author andreas.ziegler@uni-tuebingen.de. This research was partially funded by Sony AI.

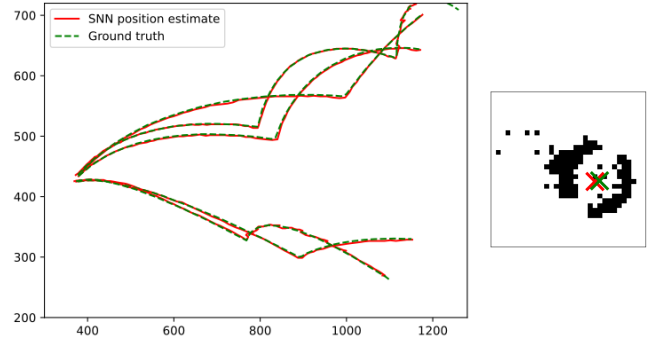


Fig. 1. (left) Five observed 2D trajectories in the camera frame of the event-based camera with ground truth in green and the estimated positions in red. (right) An example of a single 2D ball detection in a region of interest of 64x64 pixel of an accumulated event frame which serves as the input to the Spiking Neural Network (SNN) with ground truth in green and the estimated position in red.

potential. This binary output format of SNNs enables energy-efficient computations on neuromorphic hardware, since no multiplications are needed [6]. Neuromorphic hardware, specifically designed for efficient SNN processing, can leverage the sparsity and binary nature of SNN outputs.

However, efficient processing relies on gathering suitable data. Conventional cameras capture frames at a fixed frame rate, providing information about brightness and color. Event-based cameras, on the other hand, report asynchronous brightness changes per pixel, without measuring the absolute brightness [7] [8]. These cameras offer a high dynamic range, a temporal resolution in the order of μs , energy and data efficiency. The binary output of event-based cameras aligns with the spike format of SNNs, making them a good match.

While ball detection solutions with frame-based cameras are successfully used, the high temporal resolution of event-based cameras promises faster and more frequent ball detections. This can improve the prediction of the ball’s trajectory, which allows a faster robot control. SNNs align well with event data and can handle more complex scenarios, like a cluttered environment, compared to model-based solutions.

This work explores the combination of an event-based camera and SNNs for object detection and their deployment on neuromorphic edge devices. We report the error and run-time, both in simulation and on multiple neuromorphic edge devices, namely the DynapCNN¹ from SynSense, Akida² from BrainChip and Loihi2³ from Intel. Benchmarking these

¹<https://www.synsense.ai/products/dynap-cnn/>

²<https://brainchip.com/akida-enablement-platforms/>

³<https://www.intel.com/content/www/us/en/research/neuromorphic-computing-loihi-2-technology-brief.html>

three widely used neuromorphic edge devices on our use case of object detection gives an example of what is possible with these edge devices in robotics perception applications.

Contributions of this work are as follows:

- We show how event-based cameras and SNNs complement each other
- We present an object detection system for fast-moving objects, capable of running in real-time
- We show the capabilities and limitations of a deployment on three neuromorphic edge devices
- We deploy an SNN for object detection on a neuromorphic edge device in a real-time table tennis robot system
- We make the used dataset publicly available

II. RELATED WORK

We will start with an introduction to event-based cameras in Section II-A. SNNs will be covered in Section II-B. Different ways to train an SNN are covered in Section II-C and in Section II-D. We will finish the related work covering spiking object detection in Section II-E.

A. Event-Based Cameras

Event-based cameras, also known as neuromorphic cameras or dynamic vision sensors, have gained considerable attention in computer vision and robotics due to their unique characteristics and advantages over traditional frame-based cameras [7][8]. Event-based cameras operate by detecting logarithmic changes in brightness asynchronously on a per-pixel basis, reporting events only when the brightness change exceeds a specified threshold.

The asynchronous event-based nature of event-based cameras enables high temporal resolution and low latency, making them particularly suitable for capturing fast-moving objects [9][10][11] and scenes with a high dynamic range [12][13].

B. Spiking Neural Networks (SNN)

SNNs have garnered substantial interest in the field of NNs due to their biological inspiration and potential for energy-efficient computation [14]. SNNs differ from traditional Artificial Neural Networks (ANNs) by modeling the spiking behavior of biological neurons more closely. They rely on sparse and binary spikes for information processing. SNNs can represent different neuron models, such as the Integrate-and-Fire (IF) [15] or the leaky IF [16] model.

Studies indicate that SNNs are more energy-efficient [14] and excel in processing spatio-temporal data due to their use of sparse, binary signals [17]. This efficiency stems from requiring only simple additions rather than complex multiplications, reducing both computational and memory demands [6]. Consequently, SNNs are ideal for energy-sensitive hardware applications [18][19].

A significant advancement in SNN research is the development of efficient training techniques. Converting pre-trained ANNs into SNNs, will be described in Section II-C and direct training of SNNs using spike-based learning rules, in Section II-D.

C. Artificial Neural Network (ANN) to SNN Conversion

One approach to train SNNs involves converting pre-trained ANNs into SNNs [20].

This can be done by approximating the output of the Rectified Linear Unit (ReLU) non-linearity with rate-code [21]. Rate-code represents the relative frequency of spikes, obtained by replacing the ReLU with the Heaviside step function and setting a spiking threshold of one. This approximation captures the essential characteristics of the ReLU, for output activities between zero and one. ReLU outputs larger than one can not be represented by normal IF neurons, as they can at most spike once per time step. However, a multi-spike neuron model [22] allows the direct representation of the entire ReLU output space through rate-code.

D. Direct Spiking Neural Network (SNN) Training

There are two major lines of research to directly train SNNs. One is to train the model through biologically plausible local learning rules, e.g., Spike Timing Dependent Plasticity (STDP) [23][24], the other one to use so-called surrogate gradients [25]. Since STDP is not available for most of the SNN frameworks used in this work, we will focus on surrogate gradients.

Back-propagation in SNNs is akin to a specific instance of back-propagation through time (BPTT), typical for RNN training. However, the Heaviside function lacks differentiability at the threshold, and therefore, surrogate gradients are necessary for approximating gradients [25].

E. Spiking Object Detection

Object detection is a fundamental task in computer vision, and traditional approaches typically use CNNs. In recent years, there has been growing interest in exploring SNNs for object detection tasks due to their potential for improved energy efficiency and event-driven processing [18][19].

The YOLO architecture [26], a popular object detection framework, has been successfully converted into a SNN variant called Spiking-YOLO in [27].

Researchers have explored using SNNs for specific object detection tasks. In [28], SNNs were employed to predict ball trajectories using data from event-based cameras. Their approach utilized spatio-temporal filters with weights incorporating delays to capture temporal information. They also employed leaky IF neurons and trained the network using STDP.

[29] utilizes an SNN for detecting balls and pipes in a simulated environment. They used simulated neuromorphic data and designed an SNN architecture specifically tailored for detecting circles, ellipses, and lines using the Hough transform. Their approach demonstrated successful detection using the designed SNN without training, relying on hard-coded algorithms.

Although promising, SNNs for object detection still faces challenges, including higher error rates compared to CNN-based detectors. Further advancements in network architectures, training algorithms, spike-based encoding schemes, and hardware are necessary to bridge this performance

gap. Moreover, optimizing the computational and memory efficiency of SNN models is crucial for enabling real-time object detection on resource-constrained devices.

III. METHOD

We recorded a custom-made dataset to train our SNNs, which we describe in Section III-A. In this work, we used three state-of-the-art SNN frameworks and a corresponding neuromorphic edge device. For each of them, we designed an SNN architecture, conforming with their specific constraints, described in Section III-B. The training with the three SNN frameworks is covered in Section III-C.

A. Data

We describe the recording setup in Section III-A.1, followed by an explanation of how the training labels were generated in Section III-A.2. The specifications of the dataset are summarized in Table I.

TABLE I
DATASET SPECIFICATIONS

Number of samples	Training: 8630, validation: 531, test: 531
Labeled samples	Automatic labeled: 7569, manually labeled: 2123
Cameras used	Event-based: 2x Prophesee EVK4 (1280x720) Frame-based: 4x FLIR Chameleon3 (1280x1024, 140fps)
Event accumulation time	1ms
Ballgun	Butterfly Amicus Prime, ball speed 4m/s

1) *Recording setup*: We used a table tennis robot setup as introduced in [2]. The setup was extended with two event-based cameras as described in [1]. This camera system consists of four FLIR Chameleon3 frame-based cameras (140 fps, 1280x1024 pixels) and two Prophesee EVK4 event-based cameras (1280x720 pixels). Camera bias settings for the event-based camera were configured to minimize noise, and so that most events would be caused by the flying ball. The whole table tennis robot system is visualized in Fig. 2. To calibrate this camera system containing frame- and event-

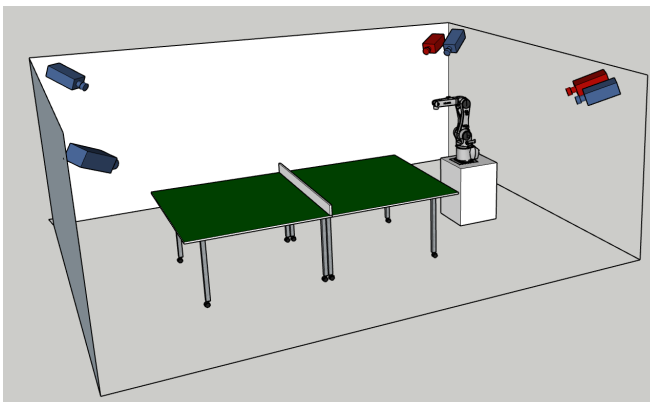


Fig. 2. Our camera setup consisting of four frame-based cameras (in blue) and two event-based cameras (in red) with baselines of 3m to 5m. Schematic is up to scale.

based cameras with baselines between 3m and 5m, we used the wand-based calibration approach introduced in [30]. The frame-based cameras are used to detect and triangulate the

position of the table tennis ball in 3D, as described in [2]. The event stream from the event-based cameras is used as input for our SNN approach.

A Butterfly Amicus Prime ball gun, with default speed settings (4m/s), was used to shoot balls in front of a static background.

2) *Data generation*: The input of our SNN is a matrix of size 64x64 pixels, where over a time range of 1ms the pixel value is set to one if at least one event occurred at the pixel and zero otherwise. This event representation removes information about the event's polarity. Keeping both polarities would require multiple input channels and, therefore, a bigger network. To achieve fast inference times, we favored smaller networks. As in [31], this event representation does also not differentiate between pixels with more or less events, as long as they have any. This reduction in information was carried out as it led to better performance in our experiments. A dynamic Region of Interest (ROI) was used to crop 64x64 pixels out of the 1280x720 pixels output of the event-based camera, similar to [2]. This was done by setting the last known ball position as the center of the ROI. This has the benefit of being applicable in real-time using the system's own past ball position estimates. Since the system starts each trajectory without past position estimates, we used manually defined start regions. This limitation could be alleviated by using the position of a frame-based detection system or an CNN based ball detector for the initialization.

The output of the SNN is the 2D pixel position of the detected ball. Therefore, the required ground truth is the 2D ball position in the image frame of the event-based camera. We used two ways to generate the 2D ball positions, serving as ground truth. We projected the triangulated 3D ball positions, which we get from the frame-based cameras using [2] into the camera frame of the event-based camera. This way, we generated 7569 ground truth positions. Since we only obtain 3D positions every 7ms, we additionally labeled the 2D ball position manually on an additional set of 2123 event frames. An example is shown in Fig. 3.



Fig. 3. An example of a manually labeled 2D ball position on an accumulated event frame (1ms accumulation time). Accumulated event frames are generated by indicating if an event occurred per pixel over a defined time interval.

B. Network Architecture

The state-of-the-art SNN frameworks and their corresponding neuromorphic edge device, we used in this work, each have their constraints. Some constraints are the input/output resolutions per layer, the number of output weights per neuron, and the type of supported layers. These constraints make it difficult to run any more complex object detection network. Therefore, the challenge was to find a trade-off between the network's complexity and the constraints and limitations of the neuromorphic edge devices.

We cast the task of detecting the table tennis ball in 2D as a classification task. This allows fewer time steps and, therefore, a faster inference time than a regression network due to the rate-code approximation. We treat the x - and y -positions as two independent classification tasks. In this case, the ball’s x -position can be one of 64 classes, as can the y -position. A visualization of the network’s output is shown in Fig. 4. Although the neuromorphic edge devices support higher input resolutions (128x128 pixels for the DynapCNN), we decided to use only 64x64 pixels to improve the inference time, which is crucial for our real-time use case. To receive the network’s prediction, the neurons with the maximal output are determined in each of the two populations.

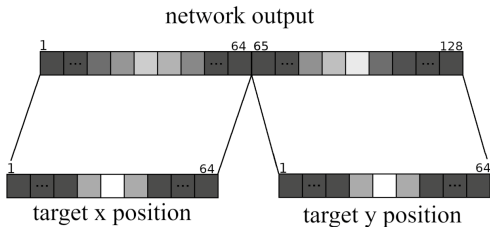


Fig. 4. The network has 128 output neurons, which are split into two populations. Each neuron in the first population represents an x -position, and each neuron in the second represents a y -position. The target is also split into an x - and y -target, each setting one as the target activity for the correct neuron, 0.5 for the two adjacent neurons, and zero for all others. Values are represented using brightness, with larger values being brighter.

The network consists of four layers, the first two being convolutional layers and the last two being linear layers. A description of the network is provided in Table II. The activation function and the pooling are given in the following order: sinabs / MetaTF / Lava. “None” indicates that no layer is used for the corresponding SNN framework. Since all the

TABLE II

NETWORK ARCHITECTURE FOR THE THREE SNN FRAMEWORKS. THE ACTIVATION FUNCTION AND THE POOLING ARE GIVEN IN THE FOLLOWING ORDER: SINABS / METATF / LAVA. “NONE” INDICATES THAT NO LAYER IS USED FOR THE CORRESPONDING SNN FRAMEWORK. WHERE STRIDE IS NOT EXPLICIT, IT DEFAULTS TO 1.

Layer	Layer Specifics
1	ConvLayer(outChannels = 4, kernelsize = 5x5, stride = 2) Multispikes IF / (BatchNorm & QuantizedReLU) / LIF AveragePool(2x2) / MaxPool(2x2) / None
2	ConvLayer(outChannels = 4, kernelsize = 3x3) Multispikes IF / (BatchNorm & QuantizedReLU) / LIF AveragePool(2x2) / None / None
3	LinearLayer(outChannels = 64) Multispikes IF / (BatchNorm & QuantizedReLU) / LIF
4	LinearLayer(outChannels = 128) Multispikes IF / None / LIF

SNN frameworks we used had different limitations, we could not use one SNN architecture for all of them. Therefore, we modified the SNN to comply with the constraints of the corresponding framework.

1) *sinabs (DynapCNN)*: While the SNN trained on the GPU processes frames and is clocked, the SNN on the DynapCNN processes events and is asynchronous. This difference leads to a gap between the two SNNs. We use the multi-spike learning approach [22] supported by sinabs, since it reduces this gap. The multispike IF neurons are followed by average pooling to further reduce network size and remain within the limits for the number of neurons per layer imposed by the DynapCNN.

2) *MetaTF (Akida)*: The network we used to train with the MetaTF framework uses batch normalization layers in all layers except the last one, as it led to improved performance, and the Brainchip supports the use of biases, which are necessary to integrate batch normalization into an SNN without significant effect on the inference time. Quantized ReLUs are used because the Akida chip squashes the rate-code approximation of the ReLU into one time step, where it is then represented by a step-wise quantized ReLU. In the first layer, we use max pooling instead of average pooling, since this is the pooling type supported by the MetaTF framework. For the use on the chip, pooling comes with additional restrictions, which is why there is no second pooling layer and instead a stride of two in the second convolutional layer.

3) *Lava (Loihi2)*: For the network trained with Lava, we use leaky IF neurons, since they are the standard neuron type supported by the Loihi2 chip and performed better than IF neurons. An increased number of channels (8, 16, 64, and 128) is used, as this was necessary to reach comparable accuracy. No pooling layers were used, as they cannot be mapped onto the Loihi2 chip.

C. Training

As mentioned in Section II-B, there are two ways to train SNNs. The conversion from an ANN to an SNN and direct SNN training. The former approach has notable drawbacks, including a typical decline in accuracy, especially when using few time steps, and a high spike rate [32]. Therefore, we used direct SNN training for the DynapCNN and Intel’s bootstrap method for Loihi2. Akida uses an equivalent representation of an SNN using a step-wise quantized ReLU, which can be trained using quantization-aware training and allows for processing in a single time step.

While the standard loss for a classification task would be the cross entropy loss, the Mean Squared Error (MSE) proved more suitable for our use case. We observed that the cross entropy loss leads to SNNs with very large activations. Large activations result in more spikes, causing more synaptic operations, making the network slower when used on edge devices. Using the MSE requires a target output of the same shape as the network output. The target that worked best was setting the correct neuron’s target output to one, the target output for the two neurons directly adjacent to 0.5, and all other neuron targets to 0, as visualized in Fig. 4.

For all SNN frameworks, we trained the networks on the GPU and deployed them on the edge devices for inference. We used all the 7569 automatically generated 2D ground

truth positions and additional 1061 manually labeled positions (as described in Section III-A.2) for the training set and 531 manually labeled 2D positions for the validation and the test set.

Since the training depends on the SNN framework, we describe the training for each one. Common hyperparameters are listed in Table III.

TABLE III
COMMON HYPERPARAMETERS OF THE SNN FRAMEWORKS.

SNN framework	Learning rate	Batch size	Optimizer
sinnabs (DynapCNN)	0.0001	200	Adam
Lava (Loihi2)	0.001	100	Adam
MetaTF (Akida)	0.0001	1000	Adam

1) *Training with sinabs (DynapCNN)*: To train SNNs for the DynapCNN, SynSense provides sinabs⁴ as a framework. We use the multi-spike learning approach [22] supported by sinabs, since it closely matches the neural behavior on the chip. The sinabs framework additionally allows for the tracking of the network’s synaptic operations, which can then be used as an additional loss term to prevent over activated neurons on the DynapCNN. With the multi-spike approach, the number of generated spikes when the membrane potential exceeds the threshold is proportional to the membrane potential.

To minimize the quantization loss, the distribution of weights needs to be such that no extreme outlier weights exist which would decrease the quantization accuracy for all other weights. To normalize the weights on the DynapCNN, we used an additional loss term using only the absolute maximum of the weights for every layer.

The SNN was trained using the periodic exponential function as surrogate function [25], with back-propagation through time (BPTT).

2) *Training with MetaTF (Akida)*: To train SNNs for the Akida, BrainChip provides MetaTF⁵ as a framework. MetaTF directly trains an ANN approximating a SNN through quantization. We followed the guidelines of the MetaTF documentation to train the SNN with MetaTF.

3) *Training with Lava (Loihi2)*: To train SNNs for the Loihi2, Intel provides Lava⁶ as a framework. Direct training is supported by Lava with an enhanced version of the SLAYER framework [33]. We followed the guidelines of the Lava documentation to train the SNN with Lava-dl. The neuron thresholds were set to 0.25 and voltage decay to 0.05.

IV. EXPERIMENTS

We performed two sets of experiments. In the first one, described in Section IV-A, we evaluate the detection error and measure the time per forward pass of the three different SNN frameworks in simulation as well as on the neuromorphic edge device. Section IV-B describes the second experiment, in which we run the SNN on a neuromorphic edge device within a table tennis robot setup in real-time.

⁴<https://github.com/synsense/sinabs>

⁵<https://doc.brainchipinc.com/index.html>

⁶<https://lava-nc.org/index.html>

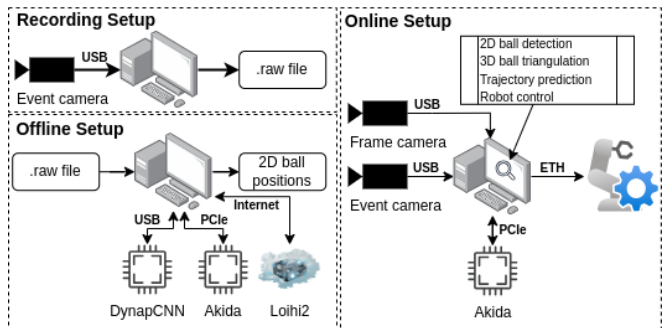


Fig. 5. (left) Experiment setup for the offline experiment. (right) Experiment setup for the online experiment.

A. Offline experiment

In this experiment, we compare the different SNN frameworks in terms of error and time per forward pass given our robotic perception task. We recorded data with the setup introduced in Section III-A. Given this recorded data, we ran the 2D ball detection 10 times for BrainChip and sinabs and 5 times for Lava. The setup is depicted in Fig. 5 on the left. Five recorded 2D ball trajectories and a single 2D ball detection are shown in Fig. 1.

The error, as well as the time per forward pass, was recorded for every run, and we report the mean and standard deviation in Table IV. Steps indicate how many time steps

TABLE IV
BALL CENTER ERROR AND TIME PER FORWARD PASS OF THE DIFFERENT SNN FRAMEWORKS AND ON THEIR CORRESPONDING NEUROMORPHIC EDGE DEVICE. STEPS INDICATE HOW MANY TIME STEPS WERE USED FOR ONE INFERENCE PASS. THE RESULTS ARE REPORTED WITH MEAN AND STD. DEV OVER MULTIPLE RUNS.

Framework	Sim	Hardware	Steps	Error [pixel]	One forward pass [ms]
BrainChip	x		15 (1)	1.44 ± 1.41	1.75 ± 0.82
BrainChip		Akida	15 (1)	1.44 ± 1.41	2.20 ± 0.35
sinabs	x		8 (1)	1.55 ± 1.89	1.59 ± 1.61
sinabs		DynapCNN	8	1.59 ± 1.83	46.04 ± 21.38
Lava	x		20	1.57 ± 1.55	1764.89 ± 1374.36
Lava		Loihi2	20	1.57 ± 1.55	1458.57 ± 230.500

were used for the rate-code for one inference pass, a trade-off between speed and accuracy. The steps count in brackets represents the number of time steps when using multispike neurons.

As can be seen in Table IV the BrainChip framework has the lowest ball center error of 1.44 pixels. The error of sinabs and Lava are 1.55 pixels and 1.57 pixels, respectively, quite close together. These errors are comparable with the frame-based ball detection approach in [34], which achieves an error of 1.32 pixels.

Important to note is that depending on the neuromorphic edge device, the total time per forward pass is heavily influenced by the integration into the system. The total time for a forward pass includes the inference time and, depending on the neuromorphic edge device data transfer, pre- and post-processing. Therefore, we list the total time per forward pass and the inference time in Table V.

TABLE V

TOTAL TIME PER FORWARD PASS AND INFERENCE TIME OF THE DIFFERENT NEUROMORPHIC EDGE DEVICES WITH MEAN AND STD. DEV OVER 10 RUNS. *PROCESSING ONE INPUT ON THE DYNAPCNN TAKES AN AVERAGE OF 1.765MS, BUT WITH DELAYS FROM THE USB CONNECTION, THE TIME FOR A FORWARD PASS IS SIGNIFICANTLY HIGHER.

Edge device	One forward pass [ms]	Inference time [ms]
BrainChip Akida	2.20 ± 0.35	0.89 ± 0.28
DynapCNN	46.04 ± 21.38*	0.82 ± 0.24
Loihi2	1458.57 ± 230.50	0.62 ± 0.01

For the BrainChip Akida, which is installed as a PCIe card, the time to load data onto the device and return the results is a relatively small overhead (0.89ms inference time and 2.20ms for a forward pass).

The DynapCNN from SynSense is connected to the PC via USB. We operate the DynapCNN in a streaming mode. This allows a fast inference time of 0.82ms but does come with a relatively high delay coming from the USB connection and other sources, which leads to 46.04ms for a forward pass. The streaming mode allows for a high data throughput with an average processing time of 1.765ms on the chip but does not remove the delay caused by the USB connection. Using the DynapCNN with another event-based camera might improve the setup and therefore, remove the mentioned delays. The recent development of combining an event-based camera with an SNN on the same chip, as the Speck⁷ from SynSense, looks promising. However, the current camera resolution of 128x128 pixels is too low for our application.

For Loihi2, we did not have direct access to an edge device, but only through a virtual machine provided by Intel via the Intel Neuromorphic Research Community⁸. With this Loihi2 setup, the time per forward pass is with 1458.57ms two orders of magnitude slower than the other devices. This is mainly due to inefficient communication between the virtual machine and the Loihi2 chip, which is a consequence of our current implementation not being well optimized in this regard.

Overall, we can see that while the errors of the different neuromorphic frameworks are quite close together, the difference in inference time and the time per forward pass varies significantly. As already mentioned, the way in which the neuromorphic edge devices are connected to the PC plays a crucial role.

B. Online (real-time) experiment

In this experiment, we integrated the SNN based ball detection into our table tennis robot system, described in Section III-A. As explained in [2], to determine the 3D position of the table tennis ball, at least two cameras need to detect the ball in order to perform triangulation. Since we only have one device for each of the three SNN frameworks,

covered in this work, we used one event-based camera with the introduced SNN ball detection together with a frame-based camera and the ball detection presented in [2]. We used the Akida PCIe card from BrainChip, since the system integration does not introduce latencies as high as the DynapCNN does, and we did not yet have access to a Loihi2 edge device. The experiment setup is depicted in Fig. 5 on the right, and the physical setup shown in Fig. 6.



Fig. 6. The table tennis robot setup with the robot hitting back a table tennis ball in a rally.

In this experiment, we shot 15 table tennis balls with a Butterfly Amicus ball gun. Since the 3D triangulation and robot arm control are not part of this work, we used the existing ones from [2]. We report the ball return rate of the robot, since controlling the landing point of the ball is out of scope for this work. Given this setup, we achieved a ball return rate of 1.0.

As previously mentioned, we used one event-based camera with the SNN based ball detection and a frame-based camera with an existing ball detection to triangulate the 3D ball position. Although our online experiment does not rely solely on our SNN based ball detection, we have shown that this would be possible, and future work could involve evaluating the system with an additional Akida PCIe card.

V. CONCLUSION

In this work, we used an event-based camera in combination with Spiking Neural Networks (SNNs) for ball detection in a table tennis robot system as a use case for a real-time perception task. Three different SNN frameworks, namely sinabs, MetaTF, and Lava, and a corresponding neuromorphic edge device (DynapCNN, Akida, and Loihi2) were used, and their errors, time per forward pass, and inference time were compared. Furthermore, we deployed one solution in an existing table tennis robot system to show the real-time capability of our proposed solution.

Despite the promise of asynchronous processing with SNNs, the current edge devices face limitations, primarily attributed to hardware integration. This could be solved by integrating a high-resolution event-based camera together with an SNN in one chip.

This work aims to provide the robotic research community with insights into the possibilities and challenges of deploying SNNs on current neuromorphic edge devices for real-time robotic applications.

⁷<https://www.synsense.ai/products/speck-2/>

⁸<https://intel-ncl.atlassian.net/wiki/spaces/INRC/overview>

REFERENCES

- [1] A. Ziegler, T. Gossard, K. Vetter, J. Tebbe, and A. Zell, "A multi-modal table tennis robot system," in *RoboLetics: Workshop on Robot Learning in Athletics @CoRL 2023*, 2023. [Online]. Available: <https://arxiv.org/abs/2310.19062>
- [2] J. Tebbe, Y. Gao, M. Sastre-Rienietz, and A. Zell, "A table tennis robot system using an industrial KUKA robot arm," in *Lecture Notes in Computer Science*. Springer International Publishing, 2019, pp. 33–45. [Online]. Available: https://doi.org/10.1007/978-3-030-12939-2_3
- [3] D. D'Ambrosio, N. Jaitly, V. Sindhwani, K. Oslund, P. Xu, N. Lazic, A. Shankar, T. Ding, J. Abelian, E. Coumans, G. Kouretas, T. Nguyen, J. Boyd, A. Iscen, R. Mahjourian, V. Vanhoucke, A. Bewley, Y. Kuang, M. Ahn, D. Jain, S. Kataoka, O. Cortes, P. Sermanet, C. Lynch, P. Sanketi, K. Choromanski, W. Gao, J. Kangaspunta, K. Reymann, G. Vesom, S. Moore, A. Singh, S. Abeyruwan, and L. Graesser, "Robotic table tennis: A case study into a high speed learning system," in *Robotics: Science and Systems XIX*. Robotics: Science and Systems Foundation, Jul. 2023. [Online]. Available: <https://doi.org/10.15607/rss.2023.xix.006>
- [4] S. Gomez-Gonzalez, Y. Nemmour, B. Schölkopf, and J. Peters, "Reliable real-time ball tracking for robot table tennis," *Robotics*, vol. 8, no. 4, p. 90, Oct. 2019. [Online]. Available: <https://doi.org/10.3390/robotics8040090>
- [5] T. Ding, L. Graesser, S. Abeyruwan, D. B. D'Ambrosio, A. Shankar, P. Sermanet, P. R. Sanketi, and C. Lynch, "Learning high speed precision table tennis on a physical robot," in *2022 IEEE/RSJ International Conference on Intelligent Robots and Systems (IROS)*. IEEE, Oct. 2022. [Online]. Available: <https://doi.org/10.1109/iros47612.2022.9982205>
- [6] D. A. Patterson and J. L. Hennessy, *Computer organization and design, revised printing, third edition*, 3rd ed., ser. The Morgan Kaufmann Series in Computer Architecture and Design. Oxford, England: Morgan Kaufmann, Aug. 2004.
- [7] P. Lichtsteiner, C. Posch, and T. Delbruck, "A 128x128 120 dB 15 us latency asynchronous temporal contrast vision sensor," *IEEE Journal of Solid-State Circuits*, vol. 43, no. 2, pp. 566–576, 2008. [Online]. Available: <https://doi.org/10.1109/jssc.2007.914337>
- [8] G. Gallego, T. Delbrück, G. Orchard, C. Bartolozzi, B. Taba, A. Censi, S. Leutenegger, A. J. Davison, J. Conradt, K. Daniilidis, and D. Scaramuzza, "Event-based vision: A survey," *IEEE Transactions on Pattern Analysis and Machine Intelligence*, vol. 44, no. 1, pp. 154–180, 2022.
- [9] M. Monforte, A. Arriandiaga, A. Glover, and C. Bartolozzi, "Exploiting event cameras for spatio-temporal prediction of fast-changing trajectories," in *2020 2nd IEEE International Conference on Artificial Intelligence Circuits and Systems (AICAS)*. IEEE, Aug. 2020. [Online]. Available: <http://dx.doi.org/10.1109/AICAS48895.2020.9073855>
- [10] A. Mitrokhin, C. Fermuller, C. Parameshwara, and Y. Aloimonos, "Event-based moving object detection and tracking," in *2018 IEEE/RSJ International Conference on Intelligent Robots and Systems (IROS)*. IEEE, Oct. 2018. [Online]. Available: <http://dx.doi.org/10.1109/IROS.2018.8593805>
- [11] B. Forrai, T. Miki, D. Gehrig, M. Hutter, and D. Scaramuzza, "Event-based agile object catching with a quadrupedal robot," in *2023 IEEE International Conference on Robotics and Automation (ICRA)*. IEEE, May 2023. [Online]. Available: <http://dx.doi.org/10.1109/ICRA48891.2023.10161392>
- [12] E. Perot, P. de Tournemire, D. Nitti, J. Masci, and A. Sironi, "Learning to detect objects with a 1 megapixel event camera," in *Advances in Neural Information Processing Systems*, H. Larochelle, M. Ranzato, R. Hadsell, M. F. Balcan, and H. Lin, Eds., vol. 33. Curran Associates, Inc., 2020, pp. 16 639–16 652. [Online]. Available: <https://proceedings.neurips.cc/paper/2020/file/c213877427b46fa96cff6c39e837ccee-Paper.pdf>
- [13] T. Stoffregen, C. Scheerlinck, D. Scaramuzza, T. Drummond, N. Barnes, L. Kleeman, and R. Mahony, *Reducing the Sim-to-Real Gap for Event Cameras*. Springer International Publishing, 2020, p. 534–549. [Online]. Available: http://dx.doi.org/10.1007/978-3-030-58583-9_32
- [14] E. Lemaire, L. Cordone, A. Castagnetti, P.-E. Novac, J. Courtois, and B. Miramond, *An Analytical Estimation of Spiking Neural Networks Energy Efficiency*. Springer International Publishing, 2023, p. 574–587. [Online]. Available: http://dx.doi.org/10.1007/978-3-031-30105-6_48
- [15] N. Brunel and M. C. W. van Rossum, "Lapicque's 1907 paper: from frogs to integrate-and-fire," *Biological Cybernetics*, vol. 97, no. 5–6, pp. 337–339, Oct. 2007. [Online]. Available: <https://doi.org/10.1007/s00422-007-0190-0>
- [16] S. Lu and F. Xu, "Linear leaky-integrate-and-fire neuron model based spiking neural networks and its mapping relationship to deep neural networks," *Frontiers in Neuroscience*, vol. 16, Aug. 2022. [Online]. Available: <http://dx.doi.org/10.3389/fnins.2022.857513>
- [17] P. Blouw, X. Choo, E. Hunsberger, and C. Elias-Smith, "Benchmarking keyword spotting efficiency on neuromorphic hardware," in *Proceedings of the 7th Annual Neuro-inspired Computational Elements Workshop*, ser. NICE '19. ACM, Mar. 2019. [Online].

- Available: <http://dx.doi.org/10.1145/3320288.3320304>
- [18] M. Davies, N. Srinivasa, T.-H. Lin, G. China, Y. Cao, S. H. Choday, G. Dimou, P. Joshi, N. Imam, S. Jain, Y. Liao, C.-K. Lin, A. Lines, R. Liu, D. Mathaikutty, S. McCoy, A. Paul, J. Tse, G. Venkataramanan, Y.-H. Weng, A. Wild, Y. Yang, and H. Wang, “Loihi: A neuromorphic manycore processor with on-chip learning,” *IEEE Micro*, vol. 38, no. 1, p. 82–99, Jan. 2018. [Online]. Available: <http://dx.doi.org/10.1109/MM.2018.112130359>
- [19] F. Akopyan, J. Sawada, A. Cassidy, R. Alvarez-Icaza, J. Arthur, P. Merolla, N. Imam, Y. Nakamura, P. Datta, G.-J. Nam, B. Taba, M. Beakes, B. Brezzo, J. B. Kuang, R. Manohar, W. P. Risk, B. Jackson, and D. S. Modha, “Truenorth: Design and tool flow of a 65 mw 1 million neuron programmable neurosynaptic chip,” *IEEE Transactions on Computer-Aided Design of Integrated Circuits and Systems*, vol. 34, no. 10, p. 1537–1557, Oct. 2015. [Online]. Available: <http://dx.doi.org/10.1109/TCAD.2015.2474396>
- [20] Y. Cao, Y. Chen, and D. Khosla, “Spiking deep convolutional neural networks for energy-efficient object recognition,” *International Journal of Computer Vision*, vol. 113, no. 1, p. 54–66, Nov. 2014. [Online]. Available: <http://dx.doi.org/10.1007/s11263-014-0788-3>
- [21] P. U. Diehl, D. Neil, J. Binas, M. Cook, S.-C. Liu, and M. Pfeiffer, “Fast-classifying, high-accuracy spiking deep networks through weight and threshold balancing,” in *2015 International Joint Conference on Neural Networks (IJCNN)*. IEEE, Jul. 2015. [Online]. Available: <http://dx.doi.org/10.1109/IJCNN.2015.7280696>
- [22] P. Weidel and S. Sheik, “Wavesense: Efficient temporal convolutions with spiking neural networks for keyword spotting,” 2021. [Online]. Available: <https://arxiv.org/abs/2111.01456>
- [23] P. U. Diehl and M. Cook, “Unsupervised learning of digit recognition using spike-timing-dependent plasticity,” *Frontiers in Computational Neuroscience*, vol. 9, Aug. 2015. [Online]. Available: <http://dx.doi.org/10.3389/fncom.2015.00099>
- [24] G.-q. Bi and M.-m. Poo, “Synaptic modifications in cultured hippocampal neurons: Dependence on spike timing, synaptic strength, and postsynaptic cell type,” *The Journal of Neuroscience*, vol. 18, no. 24, p. 10464–10472, Dec. 1998. [Online]. Available: <http://dx.doi.org/10.1523/JNEUROSCI.18-24-10464.1998>
- [25] E. O. Neftci, H. Mostafa, and F. Zenke, “Surrogate gradient learning in spiking neural networks: Bringing the power of gradient-based optimization to spiking neural networks,” *IEEE Signal Processing Magazine*, vol. 36, no. 6, p. 51–63, Nov. 2019. [Online]. Available: <http://dx.doi.org/10.1109/MSP.2019.2931595>
- [26] J. Redmon, S. Divvala, R. Girshick, and A. Farhadi, “You only look once: Unified, real-time object detection,” in *Proceedings of the IEEE Conference on Computer Vision and Pattern Recognition (CVPR)*, June 2016.
- [27] S. Kim, S. Park, B. Na, and S. Yoon, “Spiking-YOLO: Spiking neural network for energy-efficient object detection,” *Proceedings of the AAAI Conference on Artificial Intelligence*, vol. 34, no. 07, pp. 11 270–11 277, Apr. 2020. [Online]. Available: <https://doi.org/10.1609/aaai.v34i07.6787>
- [28] G. Debat, T. Chauhan, B. R. Cottreau, T. Masquelier, M. Paindavoine, and R. Baures, “Event-based trajectory prediction using spiking neural networks,” *Frontiers in Computational Neuroscience*, vol. 15, May 2021. [Online]. Available: <https://doi.org/10.3389/fncom.2021.658764>
- [29] Z. Jiang, Z. Bing, K. Huang, and A. Knoll, “Retina-based pipe-like object tracking implemented through spiking neural network on a snake robot,” *Frontiers in Neurobotics*, vol. 13, May 2019. [Online]. Available: <https://doi.org/10.3389/fnbot.2019.00029>
- [30] T. Gossard, A. Ziegler, L. Kolmar, J. Tebbe, and A. Zell, “Ewand: A calibration framework for wide baseline frame-based and event-based camera systems,” in *2024 International Conference on Robotics and Automation (ICRA)*. IEEE, 2024. [Online]. Available: <https://arxiv.org/pdf/2309.12685.pdf>
- [31] V. Vasco, A. Glover, and C. Bartolozzi, “Fast event-based harris corner detection exploiting the advantages of event-driven cameras,” in *2016 IEEE/RSJ International Conference on Intelligent Robots and Systems (IROS)*. IEEE, Oct. 2016. [Online]. Available: <http://dx.doi.org/10.1109/IROS.2016.7759610>
- [32] J. K. Eshraghian, M. Ward, E. O. Neftci, X. Wang, G. Lenz, G. Dwivedi, M. Bennamoun, D. S. Jeong, and W. D. Lu, “Training spiking neural networks using lessons from deep learning,” *Proceedings of the IEEE*, vol. 111, no. 9, p. 1016–1054, Sep. 2023. [Online]. Available: <http://dx.doi.org/10.1109/JPROC.2023.3308088>
- [33] S. B. Shrestha and G. Orchard, “Slayer: Spike layer error reassignment in time,” in *Advances in Neural Information Processing Systems*, S. Bengio, H. Wallach, H. Larochelle, K. Grauman, N. Cesa-Bianchi, and R. Garnett, Eds., vol. 31. Curran Associates, Inc., 2018. [Online]. Available: https://proceedings.neurips.cc/paper_files/paper/2018/file/82f2b308c3b01637c607ce05f52a2fed-Paper.pdf
- [34] J. Tebbe, “Adaptive robot systems in highly dynamic environments: A table tennis robot,” Ph.D. dissertation, University of Tübingen, 2021.